International Journal of the Physical Sciences Vol. 6(27), pp. 6268-6279, 2 November, 2011
Available online at http://www.academicjournals.org/IJPS
DOI: 10.5897/IJPS09.251
ISSN 1992 - 1950 ©2011 Academic Journals

Full Length Research Paper

Study of Congo red photodegradation kinetic catalyzed by $Zn_{1-X}Cu_XS$ and $Zn_{1-X}Ni_XS$ nanoparticles

H. R. Pouretedal* and M. H. Keshavarz

Faculty of Science, Malek-ashtsr University of Technology, Shahin-shahr, I. R. Iran.

Accepted 14 April, 2011

A controlled co-precipitation method was used to prepare nanoparticles of zinc sulfide doped with Ni and/or Cu in the presence of mercaptoethanol as capping agent. The nanoparticles characterize via UV-visible spectra, atomic absorption spectrophotometer (AAS), X-ray powder diffraction (XRD) patterns and transmission electron microscope (TEM) image. The doping of Ni^{2+} and/or Cu^{2+} ions did not altered the phase of zinc sulfide nanoparticles. Congo red photodegradation kinetic catalyzed by synthesized nanoparticles was studied under UV-visible irradiation. The effect of dopant mole fraction, the dosage of photocatalysts and the samples pH were investigated on the decolorization rate of dye. More degradation of dye was achieved in neutral samples versus acidic or alkaline pH. The Congo red was degraded more than 95 and 98% in the presence of 800 mg/L of $Zn_{0.94}Ni_{0.06}S$ and $Zn_{0.90}Cu_{0.10}S$ nanoparticles, respectively, within 120 min. The effect of hydrogen peroxide and several anions were investigated on the catalytic activity of proposed photocatalysts. Also, the reproducibility of nanoparticles behavior as photocatalyst showed at least a four-cycle of photodegradation process.

Key words: Nanoparticles, zinc sulfide, Congo red, photocatalyst, photodegradation.

INTRODUCTION

Textile dyes and other industrial dyestuffs constitute one of the largest groups of organic compounds which represent an increasing environmental danger. Waste waters generated by the textile industries contain considerable amounts of non-fixed dyes, especially of azo dyes, and huge amount of inorganic salts. Azo dyes with aromatic moieties linked together by azo (–N=N–) chromophores, represent the largest class of dyes used in textile processing and other industries. Approximately, 50 to 70% of the dyes are aromatic azo compounds (Molinari et al., 2004; Bilgi and Demir, 2005). It is well known that some azo dyes and their degradation products such as aromatic amines are highly carcinogenic (Konstantinou and Triantafyllos, 2004; Zhang et al., 2007). Physical methods such as adsorption, biological methods (biodegradation) and chemical methods such as chlorination and ozonation are the most frequently used methods for the removal of the textile dyes from wastewater. Others are flocculation, reverse osmosis and adsorption onto activated carbon. Since they are not destructive but only transfer the contamination from one phase to another, a different kind of pollution is faced and further treatments are required; namely, advanced oxidation processes which have been extensively investigated (Guillard et al., 2003; Augugliaro et al., 2002). Among these processes, heterogeneous photocatalysis is found as an emerging destructive technology leading to the total mineralization of most of the organic pollutants.

One of the attractive research fields in recent years is the synthesis of various sizes and shapes of semiconductor materials nanoparticles. The goal of these activities is to improve the performance and utilization of nanoparticles in various applications from sensing devices to photonic materials in molecular electronics and to advanced oxidation techniques (AOTs). The size and shape dependent optical and electronic properties of these nanoparticles make an interesting case for exploiting them in light induced chemical reactions (Hachem et al., 2001; Alaton et al., 2002).

Zinc sulfide (ZnS), which is an important wide band gap semiconductor, has attracted much attention owing to its

*Corresponding author. E-mail: HR_POURETEDAL@mut-es.ac.ir. Tel: +98-312-591-2253. Fax: +98-312-522-0420.

Abbreviations: AOTs, Advanced oxidation techniques; **AAS,** atomic absorption spectrophotometer; **XRD,** X-ray powder diffraction; **TEM,** transmission electron microscope; **CR,** Congo red; **IEP,** isoelectric points.

wide applications including UV light emitting diodes, efficient phosphors in flat-panel displays, photo voltaic devices etc (Jayanthi et al., 2007). The doping of ZnS with transition metals such as Mn, Ni, Fe and Ag is interesting to researchers because of the effect of dopant on the photoluminescence and photoreactivity properties of the semiconductor. The effect of iron as dopant in the photoluminescence of ZnS nanoparticles was shown as a blue shift of the fundamental absorption edge with increasing iron. Substitution of Zn in ZnS with Fe and Ni showed similar variation in band gap and hence particle size as well as with the dopant concentration X of these elements in $Zn_{1-X}M_XS$, while such variations on substitution with Mn are distinct, possibly because the sulfides of Zn and Mn are isostructural. Experimental results showed that there is considerable change in the photoluminescence spectra of ZnS:M nanoparticles doped with M (M = Co, Fe). Also, the lifetimes suggest a new additional decay channel of the carrier in the host material (Sambasivam et al., 2009; Shah et al., 2002).

The aim of this study is to investigate the photodegradation kinetic of Congo red (CR) catalyzed by nanoparticles of zinc sulfide doped with Ni and Cu.

EXPERIMENTAL

Materials

All chemical reagents were of analytical grade and prepared from Merck and Fluka Companies. Double distilled water was used throughput to prepare the aqueous solutions. The salts of $ZnCl_2$, $NiCl_2{\cdot}6H_2O$ and $CuCl_2{\cdot}2H_2O$ were used as source of metal ions. The sodium sulfide ($Na_2S{\cdot}9H_2O$) salt were used as precipitation reagent of metal ions. Mercaptoethanol (2-hydroxyethanthiol, $HOCH_2CH_2SH$) was applied as capping agent in the precipitation process of zinc sulfide.

The Congo red ($C_{32}H_{22}N_6Na_2O_6S_2$) stock solution with concentration of 1000 mgL^{-1} was prepared by dissolving Congo red powder (C.I. 22120) in double distilled water. Other chemicals like NaOH, HCl, Na_2CO_3, NaCl, Na_2SO_4 and isopropyl alcohol solvent used during the experiments were purchased either from Merck or Fluka Companies.

Preparation of nanoparticles

The nanoparticles of $Zn_{1-X}M_XS$ (M = Ni or Cu, X = 0, 0.02, 0.04, 0.06, 0.08 and 0.10) were prepared via co-precipitation method. 100 mL homogeneous solution 0.01 M of $ZnCl_2$ and $NiCl_2{\cdot}6H_2O$ or $CuCl_2{\cdot}2H_2O$ with mole ratio of $[M^{2+}]/[Zn^{2+}]$ = 0.00, 0.02, 0.04, 0.06, 0.08 and 0.10; and 50 mL solution of 0.1 M mercaptoethanol were added in a three-vent balloon. Then, 100 mL solution of 0.01 M sodium sulfide ($Na_2S{\cdot}9H_2O$) was added drop by drop using a decanter vessel under nitrogen atmosphere while the mixture was stirred using a magnetic stirrer vigorously at room temperature. The precipitated nanoparticles of $Zn_{1-X}M_XS$ were separated from the solution with the use of a centrifuge at 3000 to 4000 rpm within 10 to 15 min; and then washed with water and isopropyl alcohol. The cleaned powders were heated in an autoclave at temperature of 100°C within 2 h to complete evaporation of the solvent.

Characterization of nanoparticles

The UV-visible absorption spectra of 10 mM solutions of nanoparticles as sol transparent samples in isopropyl alcohol were recorded by using a UV-visible spectrophotometer Perkin-Elmer Lambda 2 at room temperature. A Diffractometer Bruker D8ADVANCE Germany with anode of Cu, wavelength: 1.5406 Å (Cu Kα) and filter of Ni was used for X-ray powder diffraction (XRD) patterns. The real content of M^{2+} ions (Ni^{2+} or Cu^{2+}) in $Zn_{1-X}M_XS$ was determined via atomic absorption spectrophotometer (AAS) AA-6200 Shimadzu. Characterization of the nanoparticles was investigated by a JEOL JEM-1200EXII transmission electron microscope (TEM) operating at 120 kV. The supporting grids were formvar-covered, carbon-coated, 200-mesh copper grids.

Photodegradation of Congo red

The bleaching of Congo red catalyzed with $Zn_{1-X}Ni_XS$ and $Zn_{1-X}Cu_XS$ nanoparticles was studied under UV-visible irradiation. A photodegradation reactor system consisted of a cylindrical Pyrex-glass cell, used to perform the experiments. A low pressure mercury vapor lamp (40 W) with radiation wavelength of 332 nm was placed in a 5 cm of Pyrex-glass cell. The photoreactor was filled with 100 ml of 5.0 to 20.0 mg/L of Congo red as pollutant and 0.1 to 1.0 g/L of nanoparticles of $Zn_{1-X}M_XS$. The temperature of the reactor was kept at 25°C using a water-cooled jacket on its outside. A magnetic stirrer was used in the reactions to ensure that the suspension of the catalyst was uniform during the course of the reaction. The samples at regular intervals using Millipore membrane filters were collected and centrifuged, to remove the nanoparticles for the determination of Congo red photodegradation.

The absorbance of Congo red samples at λ_{max} of 510 nm was measured by a UV-visible spectrophotometer Perkin-Elmer Lambda 2 using a paired 1.0 cm quartz cell. The decrease of absorbance value of samples at λ_{max} of dye after irradiation in a certain time intervals showed the rate of decolorization and therefore, photodegradation efficiency of the dye. The degradation efficiency was calculated as:

$$\%D = 100 \times [(C_o-C_t)/C_o] = 100 \times [(A_o-A_t)/A_o] \quad (1)$$

Where, C_o and C_t are the initial concentration and the concentration of dye in time of t, respectively, A_o and A_t are the initial absorbance and the absorbance of sample in time t, respectively and t is irradiation time of sample.

RESULTS AND DISCUSSION

Characterization of nanoparticles

The UV-visible spectra of ZnS, $Zn_{0.94}Ni_{0.06}S$ and $Zn_{0.90}Cu_{0.10}S$ nanoparticles are shown in Figure 1. The particles of ZnS with band gap of 3.68 eV showed an absorption peak of 337 nm in visible region (Yang et al., 2002). However, as seen from Figure 1, decreasing the particles size is due to blue shift in absorption edge. The ZnS, $Zn_{0.94}Ni_{0.06}S$ and $Zn_{0.90}Cu_{0.10}S$ nanoparticles showed absorbance maxima between 260 and 280 nm in the ultraviolet region. The band gap value corresponding to the maxima is between 4.41 to 4.75 eV. This blue shift of maxima with decrease of particles size and doping of zinc sulfide crystals with nickel (Ni^{2+}) and copper (Cu^{2+}) showed increasing band gap of prepared semiconductors (Yang et al., 2002). The radiation suitable to band gap, a

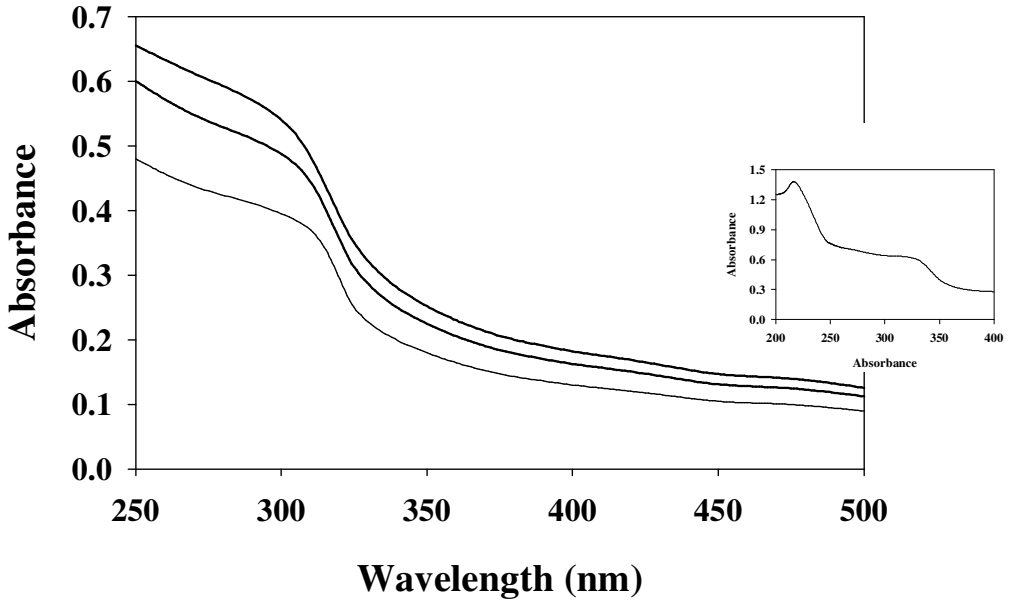

Figure 1. UV-visible spectra of ZnS, $Zn_{0.94}Ni_{0.06}S$ and $Zn_{0.90}Cu_{0.10}S$ nanoparticles in isopropyl solution from bottom to top. The inset of the figure shows the UV-visible spectra of ZnS particles.

Table 1. The real content of Ni^{2+} and Cu^{2+} in $Zn_{1-X}Ni_XS$ and $Zn_{1-X}Cu_XS$ nanoparticles, respectively.

Amount of X in $Zn_{1-X}M_XS$, predicted	Amount of Ni in $Zn_{1-X}Ni_XS$, determined	Amount of Cu in $Zn_{1-X}Cu_XS$, determined
0.02	0.015	0.017
0.04	0.034	0.035
0.06	0.056	0.054
0.08	0.073	0.072
0.10	0.090	0.091

semiconductor is due to transfer electron from valance band to capacitance band and therefore; the electrons, e^-, and the holes, h^+, are formed in valance and conductance bands, respectively. Recombination of the electrons and holes is one of the limitations of semiconductors as photocatalyst. The increasing band gap energy of a semiconductor is due to increasing life–time of electrons and holes. Thus, it is expected that photocatalyst reactivity will increase with increased life-time of electrons and holes (Qamar et al., 2005; Hoffmann et al., 1995).

The real content of Ni^{2+} and Cu^{2+} was determined by using AAS method. The amount of 0.1000 g of $Zn_{1-X}Ni_XS$ and/or $Zn_{1-X}Cu_XS$ nanoparticles dissolved in 2 M nitric acid and dilute up to ca. 100.0 mL with double distilled water. The concentration of Ni^{2+} and Cu^{2+} ions in sample solutions was determined from the absorbance and calibration curves. The results are summarized in Table 1. The obtained results indicated that, the doping of ZnS nanoparticles with Ni^{2+} and Cu^{2+} ions was carried out at the desired mole fractions (Lakshmi et al., 2009). Thus, it is possible to dope the nanoparticles at room temperature and doping in desired amount.

The X-ray diffraction of $Zn_{0.94}Ni_{0.06}S$ and $Zn_{0.90}Cu_{0.10}S$ nanosized powders in 2θ of 20 to 80° are indicated in Figure 2. The nanoparticles exhibit a zinc-bland crystal structure. The three diffraction peaks at 2θ of 29, 48 and 56° correspond to (1 1 1), (2 2 0) and (3 1 1) planes of the cubic crystalline ZnS (Warad et al., 2005). Doping of Ni^{2+} and/or Cu^{2+} ions into ZnS has not altered the phase and no trace of NiS, CuS or any other secondary phase was observed in the samples. The average of particles size was obtained about 2.0 to 10.0 nm using calculations of Debye-Scheerer relations (Guinier, 1963).

Figure 3 shows the TEM image of $Zn_{0.90}Cu_{0.10}S$ nanoparticles. The nanoparticles size of < 50 nm was confirmed by using TEM image. Nanoparticles were probably obtained through bond of sulfur end of the mercaptoethanol with sulfur in zinc sulphide. Mercaptoethanol cover particles of zinc sulphide and they do not

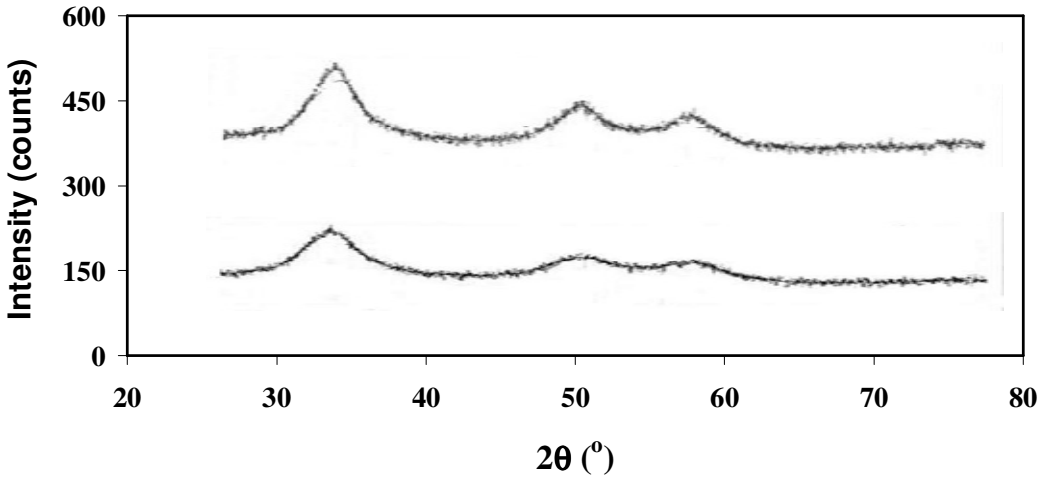

Figure 2. X-ray diffraction patterns of $Zn_{0.94}Ni_{0.06}S$ (up) and $Zn_{0.90}Cu_{0.10}S$ (down) nanocrystals.

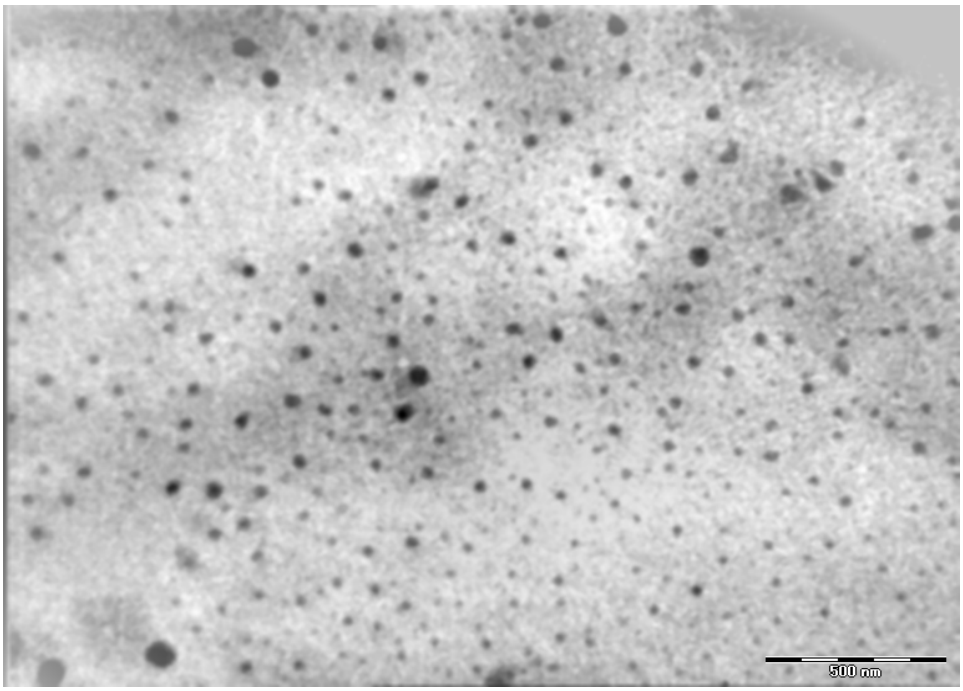

Figure 3. Transmission electron microscope (TEM) image of $Zn_{0.90}Cu_{0.10}S$ nanoparticles.

coalesce to form bigger particles, even after an extensive period of time. Particles are suspended like colloids in solutions (Zeng et al., 2007).

Photodegradation of Congo red

Figure 4 shows the photodegradation efficiency of Congo red (5.0 mg/L) within 120 min in the presence of $Zn_{1-X}Ni_XS$ and $Zn_{1-X}Cu_XS$ (X = 0, 0.02, 0.04, 0.06, 0.08 and 0.10) nanoparticles with the amount of 0.1 g/L. The $Zn_{0.94}Ni_{0.06}S$ nanoparticles indicated the more photo-reactivity in comparison with pure ZnS nanoparticles. Also, it is seen from Figure 4 that, the most degradation was obtained in the presence of $Zn_{0.90}Cu_{0.10}S$ in among of $Zn_{1-X}Cu_XS$ nanoparticles. Therefore, it is concluded that the mole fractions of 0.06 and 0.10 of Ni and Cu, respectively, are suitable for increasing the reactivity of ZnS nanoparticles.

Heterogeneous photocatalysis is a complex sequence

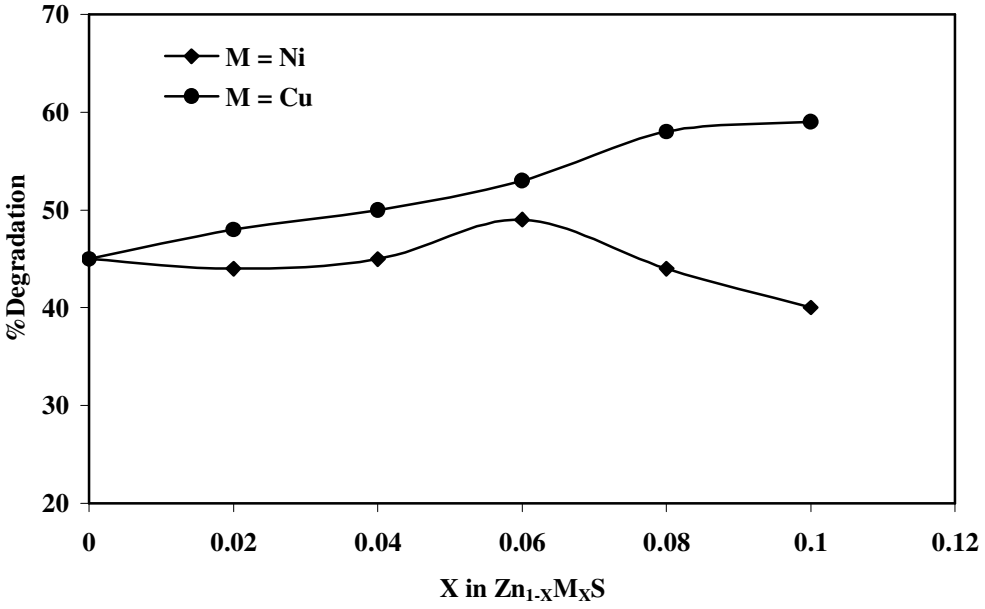

Figure 4. The effect of mole fraction of nickel and copper dopants in $Zn_{1-X}M_XS$ nanoparticles in photodegradation of Congo red in duration time of 120 min.

of reactions. The oxidation pathway is not yet fully understood. However, Pirkanniemi and Sillanpaa (2002) suggested that, the heterogeneous photocatalysis reaction followed five steps. These are: "(i) Diffusion of reactants to the surface, (ii) adsorption of reactants onto the surface, (iii) reaction on the surface, (iv) desorption of products from the surface, and (v) diffusion of products from the surface". There are two routes through which OH radicals can be formed. The reaction of the valence-band "holes" (h_{vb}^+) with either adsorbed H_2O or with the surface OH^- groups on the ZnS nanoparticle.

$$ZnS(h_{vb}^+) + H_2O_{ads} \longrightarrow ZnS + {}^{\bullet}OH_{ads} + H^+ \quad (2)$$

$$ZnS(h_{vb}^+) + OH^-_{ads} \longrightarrow ZnS + {}^{\bullet}OH_{ads} \quad (3)$$

In general, donor (D) molecules such as H_2O will adsorb and react with a hole in the valence-band and an acceptor (A) such as dioxygen will also be adsorbed and react with the electron in the conduction band (e_{cb}^-), according to Equations (4) and (5).

$$ZnS(h_{vb}^+) + D_{ads} \longrightarrow ZnS + D^+_{ads} \quad (4)$$

$$ZnS(e_{cb}^-) + A_{ads} \longrightarrow ZnS + A^-_{ads} \quad (5)$$

It is generally accepted that, oxygen plays an important role. Oxygen can trap conduction-band electrons to form superoxide ion ($O_2^{-\bullet}$), Equation (6). These superoxide ions can react with hydrogen ions (formed by splitting water), forming $HO_2^{\bullet}$.

$$ZnS(e^-_{CB}) + O_{2ads} + H^+ \longrightarrow ZnS + HO_2^{\bullet} \longrightarrow O_2^- + H^+ \quad (6)$$

H_2O_2 could be formed from $HO_2^{\bullet}$ via reactions (7).

$$ZnS(e^-_{CB}) + HO_2^{\bullet} + H^+ \longrightarrow H_2O_2 \quad (7)$$

Cleavage of H_2O_2 by one of the reactions (Equations 8, 9 and 10) may yield an OH radical.

$$H_2O_2 + h\nu \longrightarrow 2\,{}^{\bullet}OH \quad (8)$$

$$H_2O_2 + O_2^{-\bullet} \longrightarrow {}^{\bullet}OH + O_2 + OH^- \quad (9)$$

$$H_2O_2 + ZnS(e^-_{CB}) \longrightarrow ZnS + {}^{\bullet}OH + OH^- \quad (10)$$

Finally, the dye degrades by the attack of direct hole and hydroxyl species (Hu and Wang, 1999).

$$h_{vb}^+(ZnS) + dye \longrightarrow dye^{\bullet+} \longrightarrow \text{oxidation of the dye} \quad (11)$$

$${}^{\bullet}OH_{ads} + dye \longrightarrow \text{degradation of the dye} \quad (12)$$

The number and the lifetime of free carriers (electrons /holes) are particle size- and dopant-dependent. The high surface area to mass ratios of nano-particles can greatly enhance the adsorption capacities of sorbent materials. Nanotechnology is a deliberate mani-pulation of matter at size scales of less than 100 nm and holds the promise of creating new materials and devices which take advantage of unique phenomena realized at those length scales. In addition to having high specific surface areas, nanoparticles also have unique adsorption properties due to different distributions of reactive surface sites and disordered surface regions (Dhermendra et al., 2008).

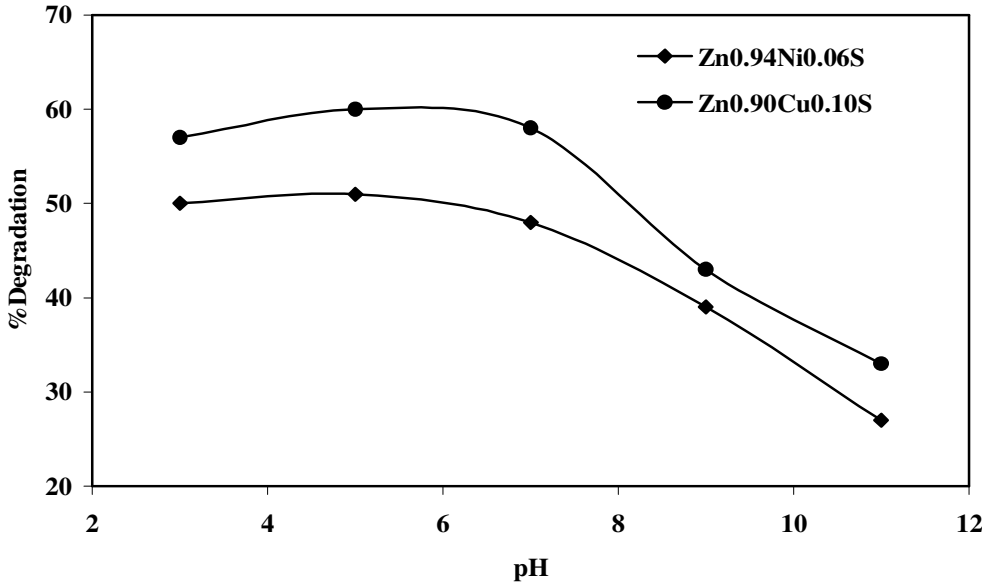

Figure 5. The effect of pH in photodegradation of Congo red catalyzed by $Zn_{0.94}Ni_{0.06}S$ and $Zn_{0.90}Cu_{0.10}S$ nanoparticles in duration time of 120 min.

There is an optimal dopant concentration that influences the reactivity of semiconductor particles. The dopants ions serve as shallow trapping sites for the charge carriers and increase the photocatalytic efficiency by separating the arrival time of e^- and h^+ at the surface. If dopant can act as a trap for both e^- and h^+, at high dopant concentration, the possibility of charge trapping is high, and as such, the charge carriers may recombine through quantum tunneling. But, if dopant acts as an h^+ trap only, the recombination of the charge carriers is not of great concern at low dopant concentrations. At high concentrations however, an h^+ may be trapped more than once as it tries to make its way to the surface. Thus, there exists an optimum dopant concentration whether the dopant acts as an e^- and h^+ trap or as an h^+ trap only (Beydoun et al., 1999).

The effect of pH samples and dosage of nanoparticles

The effect of pH samples was studied in pH range of 3 to 11 (Figure 5). The pH of the samples was adjusted using HCl and NaOH with concentrations of 1.0×10^{-2} M. As shown in Figure 5, the maximum degradation efficiency was obtained in the amplitude pH of 5 to 7 and then decreased with increasing pH. The studies of zeta (ζ) potential showed that, the isoelectric points (IEP) of ZnS semiconductor is in amplitude pH of 7.0 to 7.5 (Moignard et al., 1977). Therefore, the surfaces of photocatalysts are positively charged in acidic solutions and negatively charged in alkaline solutions. Congo red molecule with two sulfonic groups was ionized in strong acidic media and becomes a soluble Congo red anion. Therefore, in the acidic and neutral solutions, Congo red anions are easily adsorbed to ZnS nanoparticles with positive surface charge. However, at higher pH values (pH > 7), Congo red anions are generally excluded away from the negatively charged surface of ZnS nanoparticles, so degradation ratio decreases (Melghit and Al-Rabaniah, 2006).

Figure 6 illustrates photodegradation of Congo red in the different dosage of nanocatalysts of $Zn_{0.94}Ni_{0.06}S$ and $Zn_{0.90}Cu_{0.10}S$ in irradiation time of 120 min. After soaking in the dark in duration time of 30 min, the samples contained various amounts of nanoparticles irradiated for 120 min. The degradation efficiency is increased to maximum value in the presence 0.8 g/L of nanophoto-catalyst due to increase in the active sites. However, the decrease of degradation at higher catalyst loading may also be due to deactivation of activated molecules by collision with ground state molecules. At the loading amount, some parts of the photocatalyst surface become unavailable for photon absorption, and dye absorption thus bringing little stimulation to the catalytic reaction (Gözmena et al., 2009).

The effect of initial concentration of Congo red and kinetic rate constants

The photocatalytic degradation of various organic compounds such as dyes in the presence of a hetero-geneous photocatalyst can be formally described by the Langmuir-Hinshelwood kinetics model (Al-Ekabi and Serpone, 1988):

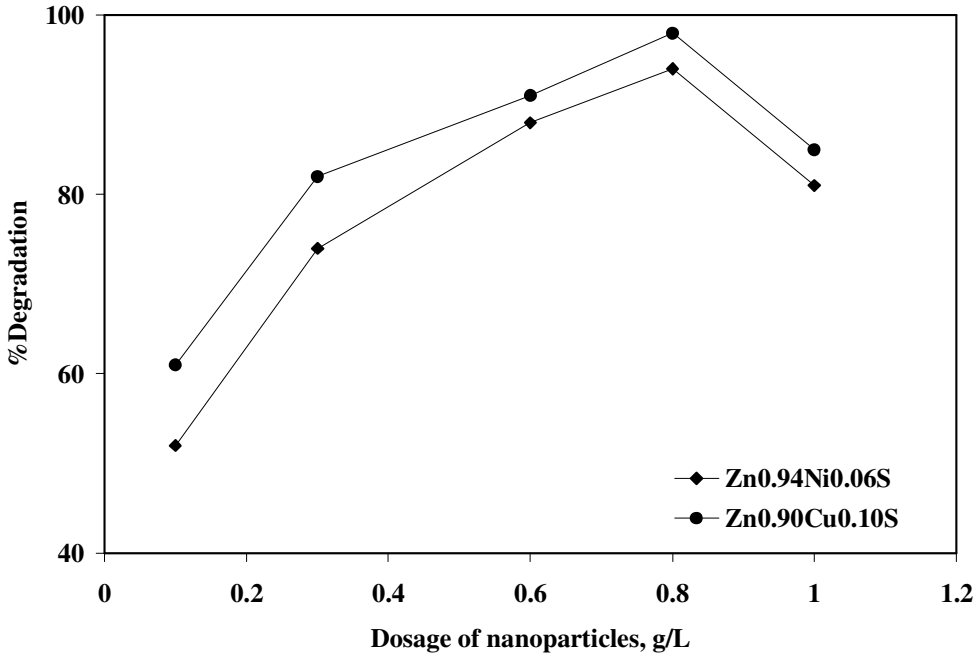

Figure 6. The effect of dosage of $Zn_{0.94}Ni_{0.06}S$ and $Zn_{0.90}Cu_{0.10}S$ nanoparticles in photodegradation of Congo red duration time of 120 min.

$$r = dC / dt = kKC /(1 + KC) \quad (13)$$

For low concentrations of dyes ($KC << 1$), neglecting KC in the denominator and integrating with respect to time t, the above equation can be simplified to the pseudo-first order kinetic model equation.

$$\ln(C_o / C_t) = kKt = K_{app} t \quad (14)$$

Where, dC/dt is the rate of dye degradation (mg/L·min), C_o and C_t are initial concentration and concentration at time t of the dye (mg/L) respectively, k is the reaction rate constant (min^{-1}), K is the adsorption coefficient of the dye onto the photocatalyst particle (L/mg) and k_{app} is the apparent rate constant calculated from the curves (min^{-1}). Figures 7 and 8 shows the degradation efficiencies of Congo red in different initial concentrations versus time catalyzed by $Zn_{0.94}Ni_{0.06}S$ and $Zn_{0.90}Cu_{0.10}S$ nanoparticles, respectively. The apparent rate constants of degradation at different initial concentrations of Congo red, k_{app}, were determined from the slope of the plots of Figures 9 and 10 in accordance to the proposed kinetic model. The apparent rate constants are given in Table 2.

As shown in Table 2, the apparent rate constants of photodegradation of Congo red decrease with increasing the initial concentration of the dye. More dye molecules were adsorbed on the surface of the catalyst as the initial concentration of dye increased, and thus the generation of hydroxyl radicals at the catalyst surface was reduced since the active sites were occupied by the dye molecules. Moreover, as the concentration of dye increase, this also caused the dye molecules to adsorb light with the result that fewer photons could reach the photocatalyst surface (Behnajady et al., 2006).

Reproducibility of the photocatalysts behavior

The degradation efficiency of Congo red in the presence of $Zn_{0.94}Ni_{0.06}S$ and $Zn_{0.90}Cu_{0.10}S$ nanoparticles during the four cycles of batch experiments is shown in Figure 10. In each step of the cycle experiments, the solution of the dye was filtered, washed and the photocatalysts were dried. The dried catalysts were used for the degradation of the dye under similar conditions. The decrease of the degradation yield of Congo red after four cycles was found to be 10%.

In other words, the loss of Zn^{2+} ions to solutions as a result of dissolution of photocatalyst was calculated by the determination of zinc ions in filtrate solutions using AAS method. With the initial amounts of $Zn_{0.94}Ni_{0.06}S$ and $Zn_{0.90}Cu_{0.10}S$ photocatalysts (0.8 g/L), only less than 0.5% loss of zinc was seen after four cycles of reusing them.

Effect of H_2O_2 concentration

The rate of Congo red (20 mg/L) photodegradation catalyzed by nanoparticles was investigated in the presence of hydrogen peroxide. The obtained results (Figure 12) showed that, the rate of degradation was increased

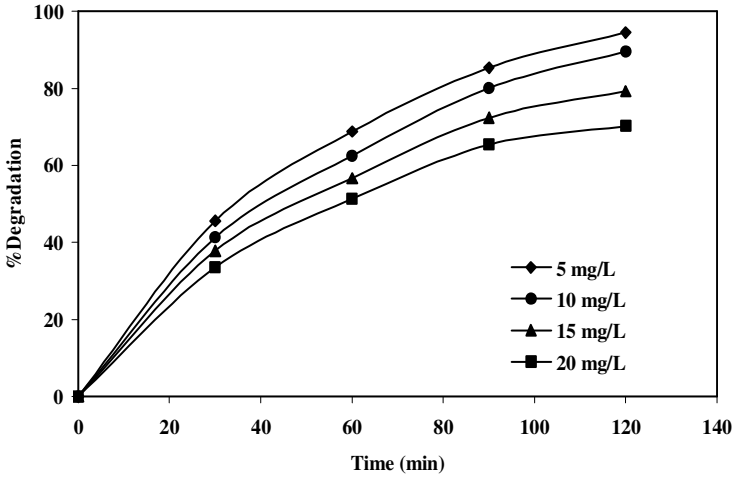

Figure 7. The effect of initial concentration of Congo red on the degradation efficiency in the presence of $Zn_{0.94}Ni_{0.06}S$ nanoparticles (0.8 g/L) at pH 5.

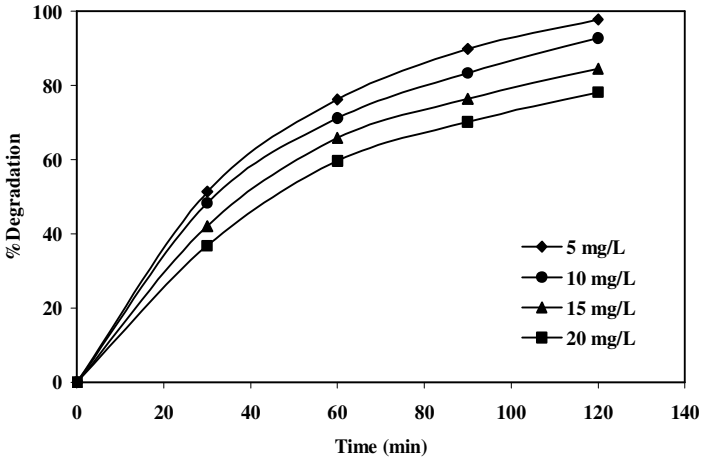

Figure 8. The effect of initial concentration of Congo red on the degradation efficiency in the presence of $Zn_{0.90}Cu_{0.10}S$ nanoparticles (0.8 g/L) at pH 5.

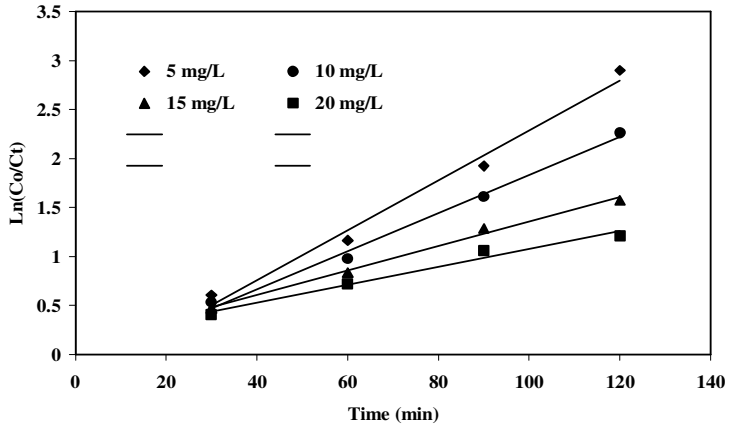

Figure 9. Kinetic data of photodegradation of Congo red in the presence of $Zn_{0.94}Ni_{0.06}S$ nanoparticles.

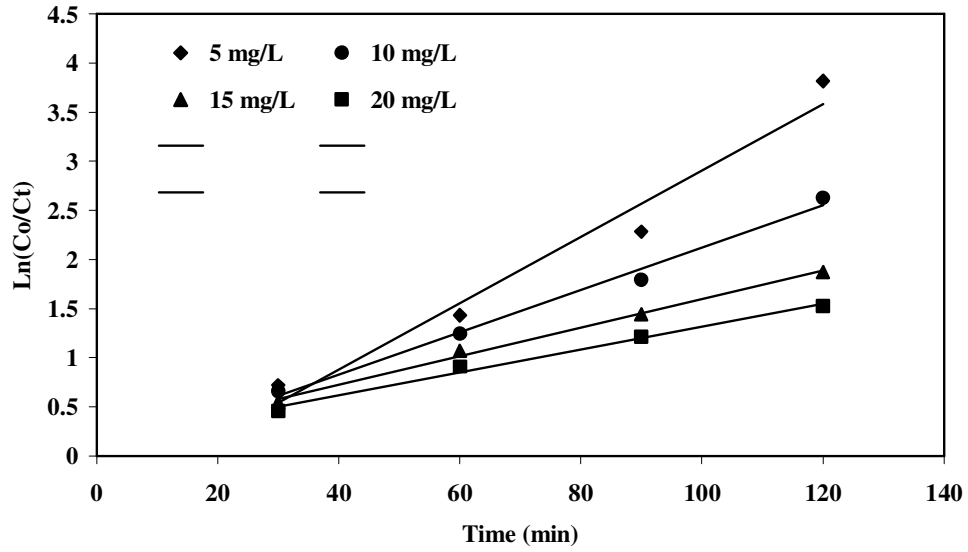

Figure 10. Kinetic data of photodegradation of Congo red in the presence of $Zn_{0.90}Cu_{0.10}S$ nanoparticles.

Table 2. Apparent rate constants, k_{app} (min^{-1}), of degradation of Congo red at different initial concentrations in the presence of $Zn_{0.94}Ni_{0.06}S$ and $Zn_{0.90}Cu_{0.10}S$ nanoparticles.

$C_{congo\ red}$ (mg/L)	$Zn_{0.94}Ni_{0.06}S$	$Zn_{0.90}Cu_{0.10}S$
5	25.5×10^{-3}	33.8×10^{-3}
10	19.4×10^{-3}	21.5×10^{-3}
15	12.5×10^{-3}	14.5×10^{-3}
20	9.2×10^{-3}	11.6×10^{-3}

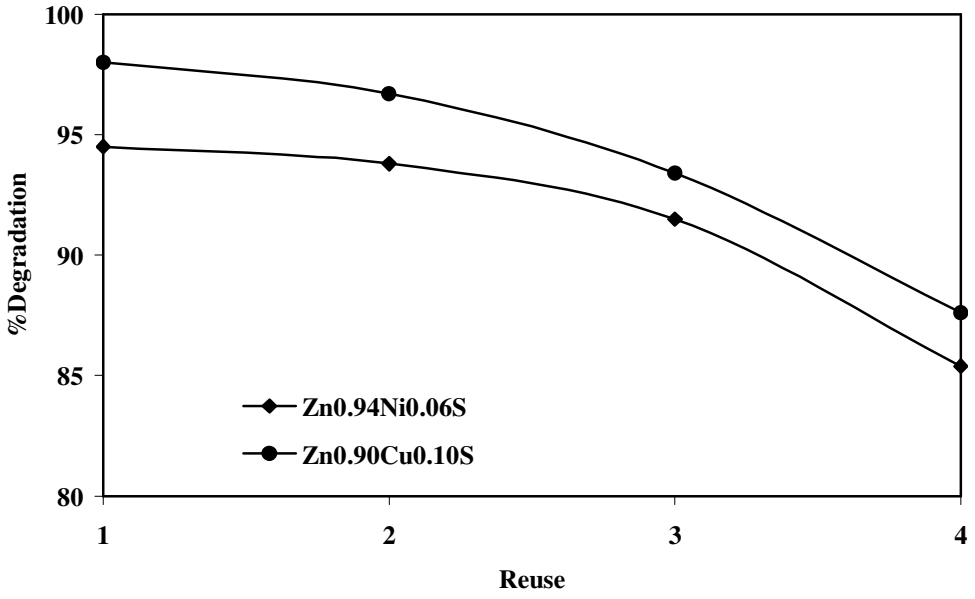

Figure 11. Reproducibility behavior of $Zn_{0.94}Ni_{0.06}S$ and $Zn_{0.90}Cu_{0.10}S$ nanoparticles as photocatalyst in photodegradation of Congo red.

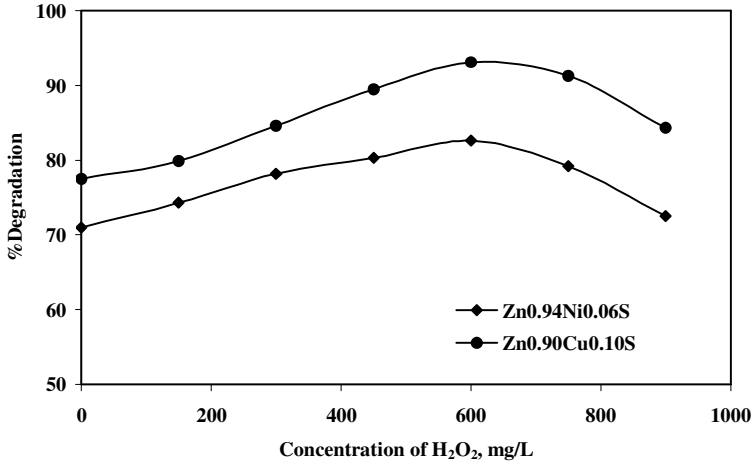

Figure 12. The effect of H_2O_2 concentration on the photodegradation of Congo red (20 mg/L) catalyzed by $Zn_{0.94}Ni_{0.06}S$ and $Zn_{0.90}Cu_{0.10}S$ nanoparticles (0.80 g/L) at pH 5 in duration time 120 min.

with increasing concentration of H_2O_2 from 0 to 600 mg/L and then decreased in higher concentrations of H_2O_2. The oxygen and/or hydrogen peroxide can be due to improved rate of photocatalytic degradation of organic compounds. The radical reaction mechanisms of photodegradation can be used for explanation of this dual effect of hydrogen peroxide. In lower concentrations, the added H_2O_2 accelerated the reaction by producing hydroxyl radicals from scavenging the electrons and absorption of UV-light by the following reactions:

$$H_2O_2 + e^- \longrightarrow {}^{\bullet}OH + OH^- \quad (15)$$

$$H_2O_2 + O_2^{-\bullet} \longrightarrow {}^{\bullet}OH + OH^- + O_2 \quad (16)$$

$$H_2O_2 + h\nu \longrightarrow 2\,{}^{\bullet}OH \quad (17)$$

However, in higher concentrations of H_2O_2, it acts as hydroxyl radical or hole scavenger to form the perhydroxyl radicals ($HO_2^{\bullet}$) which is a much weaker oxidant than hydroxyl radicals (Zhao et al., 2004).

$$H_2O_2 + {}^{\bullet}OH \longrightarrow H_2O + HO_2^{\bullet} \quad (18)$$

$$H_2O_2 + h^+ \longrightarrow H^+ + HO_2^{\bullet} \quad (19)$$

Thus, the photodegradation rate of Congo red reduced in higher concentrations of hydrogen peroxide (> 600 mg/L) by competing with H_2O_2 and dye for available hydroxyl radicals.

Effect of anions

The photodegradation efficiency of Congo red was studied in the presence of anions such as carbonate, sulfate and chloride in similarity with the real samples of the dye industry. The results for Congo red (10 mg/L) degradation catalyzed by $Zn_{0.94}Ni_{0.06}S$ and $Zn_{0.90}Cu_{0.10}S$ nanoparticles are shown in Figures 12 and 14, respectively. As shown in Figures 13 and 14, the degradation efficiencies of dye decrease with increasing concentration of CO_3^{2-}, SO_4^{2-} and Cl^- anions. The reduction of dye degradation is due to two reasons. Firstly, these anions could block the surface of heterogeneous catalysts and therefore, the active sites of catalysts were decreased for absorption of dye and intermediate molecules. Secondly, these anions could act as hydroxyl radical's scavengers (Bekbolet and Balcioglu, 1996).

$$CO_3^{2-} + {}^{\bullet}OH \longrightarrow CO_3^{-\bullet} + OH^- \quad (20)$$

$$SO_4^{2-} + {}^{\bullet}OH \longrightarrow SO_4^{-\bullet} + OH^- \quad (21)$$

$$Cl^- + {}^{\bullet}OH \longrightarrow Cl^{\bullet} + OH^- \quad (22)$$

Although, the products of the reactions of equations 20 to 22 are radicals and hydroxide ions, the oxidation potentials of produced radicals are less positive than that of the hydroxyl radicals.

Conclusion

A simple controlled-precipitation method can be applied to prepare $Zn_{1-X}M_XS$ nanoparticles with Ni and/or Cu dopants. The prepared nanoparticles showed a catalytic activity in Congo red photodegradation process. The mole fractions of 0.06 and 0.10 for nickel and copper, respectively, in $Zn_{1-X}M_XS$ nanoparticles with dosage of 0.80 g/L showed the most degradation at pH 5 within 120 min. The kinetic rate constants of degradation were

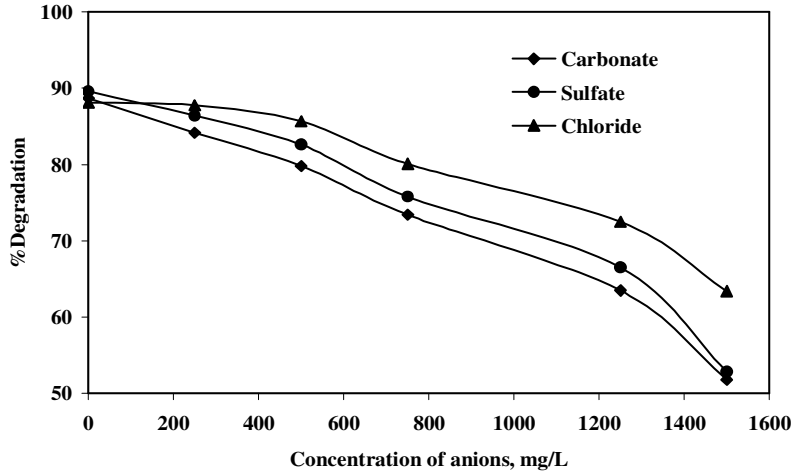

Figure 13. The effect of anions on the photodegradation of Congo red (10 mg/L) catalyzed by $Zn_{0.94}Ni_{0.06}S$ nanoparticles (0.80 g/L) at pH 5 in duration time 120 min.

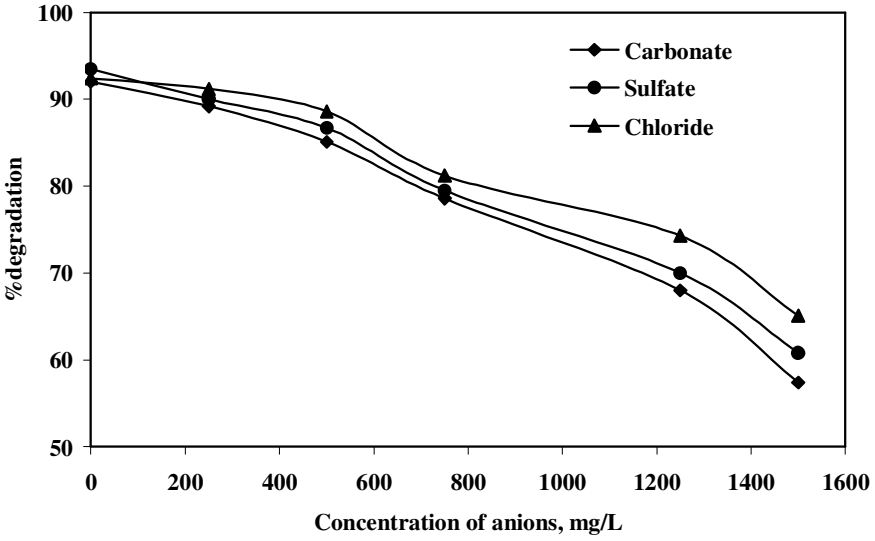

Figure 14. The effect of anions on the photodegradation of Congo red (10 mg/L) catalyzed by $Zn_{0.90}Cu_{0.10}S$ nanoparticles (0.80 g/L) at pH 5 in duration time 120 min.

decreased with increasing initial concentration of Congo red. The degradation efficiencies decrease in the presence of anions that are usually in real water samples. A 20% addition in degradation efficiency was observed in the presence of 600 mg/L hydrogen peroxide as an oxidant.

REFERENCES

Alaton IA, Balcıo˘glu IA, Bahnemann DW (2002). Advanced oxidation of a reactive dyebath effluent: comparison of O_3, H_2O_2/UV-C and TiO_2/UV-A processes. Water Res., 36: 1143-1154.

Al-Ekabi H, Serpone N (1988). Kinetic Studies in Heterogeneous Photocatalysis. J. Phys. Chem., 92: 5726-5731.

Augugliaro V, Baiocchi C, Prevot AB, Lopez EG, Loddo V, Malato S, Marci G, Palmisano L, Pazzi M, Pramauro E (2002). Azo-dyes photocatalytic degradation in aqueous suspension of TiO_2 under solar irradiation. Chemosphere, 49: 1223-1230.

Behnajady MA, Modirshahla N, Hamzavi R (2006). Kinetic study on photocatalytic degradation of C.I. Acid Yello 23 by ZnO photocatalyst. J. Hazard. Mater. 133: 226-232.

Bekbolet M, Balcioglu I (1996). Photocatalytic degradation kinetics of humic acids in aqueous TiO_2 dispersions: The influence of hydrogen peroxide and bicarbonate ion. Water Sci. Technol., 34: 73-80.

Beydoun D, Amal R, Low G, McEvoy S (1999). Role of nanoparticles in photocatalysis. J. Nanoparticle. Res., 1: 439-458.

Bilgi S, Demir C (2005). Identification of photooxidation degradation products of C. I. Reactive Orange 16 dye by gas chromatography–mass spectrometry. Dyes Pigments, 66: 69-76.

Dhermendra K, Tiwari J, Behari J, Sen P (2008). Application of Nano-particles in Waste Water Treatment. World Appl. Sci. J., 3: 417-433.

Gözmena B, Turabik M, Hesenov A (2009). Photocatalytic degradation of Basic Red 46 and Basic Yellow 28 in single and binary mixture by UV/TiO_2/periodate system. J. Hazardous Mate., 164: 1487–1495.

Guillard C, Lachheb H, Houas A, Ksibi M, Elaloui E, Herrmann JM (2003). Influence of chemical structure of dyes of pH and of inorganic salts on their photocatalytic degradation b TiO2 comparison of the efficiency of powder and supported TiO_2. J. Photochem. Photobiol. A. Chem. 158: 27-36.

Guinier A (1963). X-ray Diffraction, San Francisco, CA.

Hachem C, Bocquillon F, Zahraa O, Bouchy M (2001). Decolourization of textile industry wastewater by the photocatalytic degradation process. Dyes Pigments 49: 117-125.

Hoffmann MR, Martin ST, Choi W, Bahnemann DW (1995). Environmental applications of semiconductor photocatalysis. Chem. Rev., 95: 69-85.

Hu C, Wang YZ (1999). Decolorization and biodegradability of photocatalytic treated azo dyes and wool textile wastewater. Chemosphere, 39: 2107-2115.

Jayanthi K, Chawla S, Chander H, Haranath D (2007). Structural, optical and photoluminescence properties of ZnS: Cu nanoparticle thin films as a function of dopant concentration and quantum confinement effect. Cryst. Res. Technol., 42: 976–982.

Konstantinou KI, Triantafyllos AA (2004). TiO_2-assisted photocatalytic degradation of azo dyes in aqueous solution: kinetic and mechanistic investigations. Appl. Catal. B. Env., 49: 114.

Lakshmi PVB, Raj KS, Ramachandran K (2009). Synthesis and characterization of nano ZnS doped with Mn. Cryst. Res. Technol., 44: 153-158.

Melghit K, Al-Rabaniah SS (2006). Photodegradation of Congo red under sunlight catalysed by nanorod rutile TiO_2. J. Photochem. Photobio. A. Chem., 184: 331-334.

Moignard MS, James RO, Healy TW (1977). Adsorption of calcium at the zinc sulphide-water interface. Australian J. Chem. 30: 733-740.

Molinari R, Pirillo F, Falco M, Loddo V, Palmisano L (2004). Photocatalytic degradation of dyes by using a membrane reactor. Chem. Eng. Process., 43(9): 1103-1114.

Pirkanniemi K, Sillanpaa M (2002). Heterogeneous water phase catalysis as an environmental application: Rev. Chemosphere, 48: 1047-1060.

Qamar M, Saquib M, Muneer M (2005). Titanium dioxide mediated photocatalytic degradation of two selected azo dye derivatives, chrysoidine R and acid red 29 (chromotrope 2R), in aqueous suspensions. Desalination, 186: 255-271.

Shah SL, Li W, Huang CP, Jung O, Ni C (2002). Study of Nd^{3+}, Pd^{2+}, Pt^{4+} and Fe^{3+} dopants effect on the photoreactivity of TiO_2 nanoparticles. Colloquium, 99: 6482-6486.

Sambasivam S, Reddy BK, Divya A, Madhusudhana Rao N, Jayasankar CK, Sreedhar B (2009). Optical and ESR studies on Fe doped ZnS nanocrystals. Physics Letters A., 373: 1465-1468.

Warad HC, Ghosh SC, Hemtanon B, Thanachayanont C, Dutta J (2005). Luminescent nanoparticles of Mn doped ZnS passivated with sodium hexametaphosphate. Sci. Tech. Advanced Mater., 6: 296-301.

Yang P, Lu M, Xu D, Yang D, Chang J, Zhou G, Pan M (2002). Strong green luminescence of Ni^{2+}-doped ZnS nanocrystals. Appl. Phys. A., 74: 257-259.

Zeng HZ, Qiu KQ, Du YY, Li WZ (2007). A new way to synthesize ZnS nanoparticles. Chinese Chem. Lett., 18: 483-486.

Zhang Z, Shan Y, Wang J, Ling H, Zang S, Gao W, Zhao Z, Zhang H (2007). Investigation on the rapid degradation of Congo Red catalyzed by activated carbon powder under microwave irradiation. J. Hazard. Mater., 147: 325-333.

Zhao H, Xu S, Zhong J, Bao X (2004). Kinetic study on the photo-catalytic degradation of pyridine in TiO_2 suspension systems. Catal. Today, 93(95): 857-861.